Journal of Solid State Chemistry **154,** 317–320 (2000)
doi:10.1006/jssc.2000.8856, available online at http://www.idealibrary.com on IDEAL®

Crystal Growth and Characterization of the (Y, *RE*)$Al_3(BO_3)_4$ Solid Solutions (*RE* = Nd, Gd, Ho, Yb, Lu)

E. V. Koporulina,* N. I. Leonyuk,* A. V. Mokhov,† and O. V. Pilipenko*

*Moscow State University, 119899 Moscow, Russian Federation; and †Institute of Ore Deposits Geology, Petrography, Mineralogy and Geochemistry, 109017 Moscow, Russian Federation

Received September 9, 1999; in revised form May 31, 2000; accepted June 5, 2000

($RE Y_{1-x}$)$Al_3(BO_3)_4$ (*RE* = Nd, Gd, Ho, Yb, and Lu) single crystals were grown from fluxed melts based on the potassium trimolybdate. The compounds, morphology, and structure of these crystals were studied. The average *RE* distribution coefficients were found to be 0.35 to 1.02 for different rare-earth elements. The (Gd_xY_{1-x})$Al_3(BO_3)_4$ and $Nd_xY_{1-x}Al_3(BO_3)_4$ unit cell parameters depend on the crystal compositions according to the Vegard rule. © 2000 Academic Press

Key Words: **flux growth; rare-earth aluminum borates; solid solutions.**

INTRODUCTION

Borate crystals with the general formula $RAl_3(BO_3)_4$ (RAB) (*RE* = Y, La–Lu) can be considered polyfunctional materials with device potential due to their good thermal and chemical stability and a possibility of wide isomorphous substitutions. Most of them belong to the huntite type of structure with *R*32 space group (low RAB) (1), but Nd-, Gd-, Sm-, Eu-, and Pr-borates also have high-temperature monoclinic modifications (high RAB) with phase transition temperatures of 880–900°C, 1040–1050°C, 1130–1150°C, 1130–1150°C, and 1080°C, respectively (2–4). Of this borate family, the noncentrosymmetric $RE_xY_{1-x}Al_3(BO_3)_4$ (REYAB) crystals with $RE = Nd^{3+}$ and Er^{3+} are of most interest as promising materials for lasing and nonlinear optical applications (5–8). Optical characteristics of this borate system with $RE = Gd^{3+}$ and Eu^{3+} have been reported in Refs. (9–11). These properties strongly depend on the quality and structural characteristics of grown crystals. Among a number of publications on crystal growth and characterization of these borate compounds (for example, see Refs. (12–16)), there have practically never been systematic investigations of composition, homogeneity, morphology, or structural characteristics of the above solid solutions depending on the flux growth conditions. In the present work from this point of view we consider the system (*RE*, Y)$Al_3(BO_3)_4$, where *RE* = Nd, Gd, Ho, Yb, and Lu.

EXPERIMENTAL DETAILS

The crystals of $Nd_xY_{1-x}Al_3(BO_3)_4$, $x = 0.05, 0.1, 0.6, 0.65, 0.7$, and 0.75 (NYAB); $Gd_xY_{1-x}Al_3(BO_3)_4$, $x = 0.1, 0.2, 0.3, 0.4, 0.6, 0.65, 0.7$, and 0.75 (GYAB); $Nd_xGd_{1-x}Al_3(BO_3)_4$, $x = 0.2$ (NGAB), $Ho_xY_{1-x}Al_3(BO_3)_4$, $x = 0.01$, 0.03, and 0.05 (HYAB); $Yb_xY_{1-x}Al_3(BO_3)_4$, $x = 0.005$, 0.025, and 0.05 (YbYAB), and (Lu_xY_{1-x})$Al_3(BO_3)_4$, $x = 0.005$, 0.025, and 0.05 (LYAB) were prepared by the TSSG (top seeded solution growth) method as well as spontaneous nucleation using a $K_2Mo_3O_{10}$-based flux. The starting composition of the melts was 20 wt% *RE*YAB–80 wt% ($K_2Mo_3O_{10}$–(*RE*, Y)$_2O_3$–B_2O_3) (*RE* = Nd, Ho) or 20 wt% *RE*YAB–80 wt% ($K_2Mo_3O_{10}$–B_2O_3) (*RE* = Gd, Yb, and Lu). In the run of spontaneous crystallization, platinum crucibles with the starting mixture were kept at 1050–1120°C for 1–4 h and cooled down to 900°C at a rate of 0.2–0.5°C/h (4.8–12°C/day). Then the temperature was lowered to 350°C at the rate of 10°C/h. In the case of TSSG, the crystallization process was carried out in the temperature range of 1070–1010°C at the rate of 0.2–5°C/day following the experimental data on the solubility and the crystallization kinetics (4).

Starting chemicals for the growth of *RE*YAB crystals were as follows Y_2O_3 (99.994 wt%), Nd_2O_3 (99.935 wt%), Gd_2O_3 (99.93 wt%), Yb_2O_3 (99.93 wt%), Ho_2O_3 (99.94 wt%), Al_2O_3 (99.99 wt%), B_2O_3 (99.99 wt%), but $K_2Mo_3O_{10}$ was previously synthesized at 650°C using K_2MoO_4 (99.99 wt%) and H_2MoO_4 (99.99 wt%).

The composition of grown crystals has generally been studied by the analytical scanning electron microscope (ASEM) JSM-5300 m + Link ISIS with the accuracy of 0.2–0.3 wt%. In the case of crystals with small dopant concentrations, however, a Cameca analyzer has been used. The accuracy of these special measurements was up to 0.02–0.03 wt%.

0022-4596/00 $35.00

TABLE 1
Microprobe Analysis of REYAB Crystals

REYAB composition in fluxed melt	Average REYAB crystal composition	Average RE distribution coefficient (K)
$(Nd_{0.05}Y_{0.95})Al_3(BO_3)_4$[a]	$(Nd_{0.02}Y_{0.98})Al_3(BO_3)_4$	0.42
$Nd_{0.06}Y_{0.94}Al_3(BO_3)_4$[b]	$(Nd_{0.02}Y_{0.98})Al_3(BO_3)_4$	0.35
$(Nd_{0.1}\ Y_{0.9})Al_3(BO_3)_4$[a]	$(Nd_{0.08}Y_{0.92})Al_3(BO_3)_4$	0.82
$(Nd_{0.6}Y_{0.4})Al_3(BO_3)_4$[b]	$(Nd_{0.41}Y_{0.59})Al_3(BO_3)_4$	0.68
$(Nd_{0.65}Y_{0.35})Al_3(BO_3)_4$[b]	$(Nd_{0.59}Y_{0.41})Al_3(BO_3)_4$	0.92
$(Nd_{0.7}Y_{0.3})Al_3(BO_3)_4$[b]	$(Nd_{0.66}Y_{0.34})Al_3(BO_3)_4$	0.94
$(Nd_{0.75}Y_{0.25})Al_3(BO_3)_4$[b]	$(Nd_{0.71}Y_{0.29})Al_3(BO_3)_4$	0.94
$(Gd_{0.2}Y_{0.8})Al_3(BO_3)_4$[b]	$(Gd_{0.19}Y_{0.81})Al_3(BO_3)_4$	0.93
$(Gd_{0.3}Y_{0.7})Al_3(BO_3)_4$[b]	$(Gd_{0.29}Y_{0.69})Al_3(BO_3)_4$	0.96
$(Gd_{0.4}Y_{0.6})Al_3(BO_3)_4$[b]	$(Gd_{0.38}Y_{0.52})Al_3(BO_3)_4$	0.95
$(Gd_{0.6}Y_{0.4})Al_3(BO_3)_4$[b]	$(Gd_{0.59}Y_{0.41})Al_3(BO_3)_4$	0.98
$(Gd_{0.7}Y_{0.3})Al_3(BO_3)_4$[b]	$(Gd_{0.68}Y_{0.32})Al_3(BO_3)_4$	0.97
$(Gd_{0.75}Y_{0.25})Al_3(BO_3)_4$[b]	$(Gd_{0.72}Y_{0.28})Al_3(BO_3)_4$	0.96
$(Ho_{0.01}Y_{0.99})Al_3(BO_3)_4$[b]	$(Ho_{0.01}Y_{0.99})Al_3(BO_3)_4$	1.0
$(Ho_{0.03}Y_{0.97})Al_3(BO_3)_4$[b]	$(Ho_{0.03}Y_{0.97})Al_3(BO_3)_4$	1.00
$(Ho_{0.05}Y_{0.95})Al_3(BO_3)_4$[b]	$(Ho_{0.051}Y_{0.949})Al_3(BO_3)_4$	1.01
$(Yb_{0.005}Y_{0.995})Al_3(BO_3)_4$[b]	$(Yb_{0.0047}Y_{0.953})Al_3(BO_3)_4$	0.94
$(Yb_{0.025}Y_{0.975})Al_3(BO_3)_4$[b]	$(Yb_{0.026}Y_{0.974})Al_3(BO_3)_4$	1.02
$(Yb_{0.05}Y_{0.95})Al_3(BO_3)_4$[b]	$(Yb_{0.046}Y_{0.954})Al_3(BO_3)_4$	0.98
$(Lu_{0.05}Y_{0.95})Al_3(BO_3)_4$[b]	$(Lu_{0.05}Y_{0.95})Al_3(BO_3)_4$	1.0
$(Lu_{0.025}Y_{0.975})Al_3(BO_3)_4$[b]	$(Lu_{0.024}Y_{0.976})Al_3(BO_3)_4$	0.98

[a] TSSG.
[b] Spontaneous crystallization.

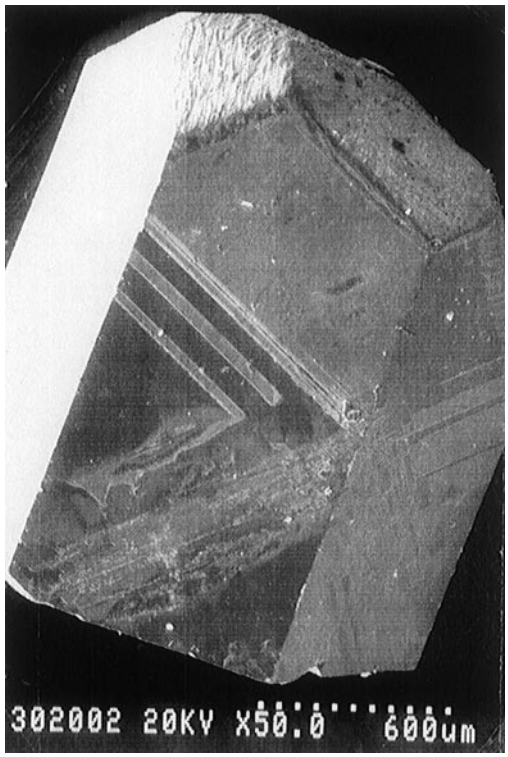

FIG. 1. Growth striation on the prism faces of $(Gd_xY_{1-x})Al_3(BO_3)_4$ ($x = 0.75$).

The *RE* distribution coefficients of Y, Nd, Gd, Ho, and Lu were calculated using the following equation $K = C_{cryst}/C_{diss} \cdot REAB$, where C_{cryst} and $C_{diss} \cdot REAB$ are *RE* concentrations in *RE*YAB-grown crystals and in the borate crystalline substances of the fluxed melt, respectively. Structural investigations of solid solutions have been performed using a Philips PW 1100 single-crystal diffractometer (Mo$K\alpha$ radiation).

RESULTS AND DISCUSSION

It was found that the average *RE* distribution coefficients varies from 0.35 to 0.94 in NYAB to 1.02 in YbYAB crystals (Table 1). A main reason for distribution coefficient variations is a difference in Y^{3+} and RE^{3+} cation sizes. In the case of NYAB, when the Nd^{3+} cation radius is considerably longer than that of Y^{3+}, it can be concluded that yttrium sites in $YAl_3(BO_3)_4$ (YAB) huntite structures are not ideally suitable for neodymium. In contrast to those, the distribution coefficients of Gd, Lu, Yb, and Ho are close to one as a consequence of minor difference in the sizes of Y^{3+} and dopant *RE* cations.

The SEM photographs showed the growth striations, which are strongly developed on the trigonal prism faces of some NYAB and GYAB crystals obtained by spontaneous nucleation (Fig. 1). These striations are parallel to the edges of $\{10\ \bar{1}1\}$ rhombohedron, and these edges also are in the plane of trigonal prism faces. In the same direction, following to the ASEM measurements, there is a sharp alteration of the layers enriched in Gd (or Nd) and the layers depleted of these *RE* elements (Fig. 2; Table 2). Since the experiments were carried out at 1120–900°C, i.e., in the range of $NdAl_3(BO_3)_4$ (NAB) and $GdAl_3(BO_3)_4$ (GAB) phase transition temperatures, it is therefore not excluded, the layers enriched in Gd and Nd belong to the high-temperature monoclinic ($C2$ or $C2/c$ space groups) type of GAB and NAB structures (2,3). On the other hand, the layers enriched in Y have rombohedral YAB structure ($R32$ space group) (1). This assumption is also based on specific features of the YAB, NAB, and GAB polytypes (17). For example, it was established that the layers of rare-earth prisms $[REAlB_2O_{10}]_{\infty\infty}$ and aluminum octahedra $[Al_2B_2O_{10}]_{\infty\infty}$ alternate along the $[10\ \bar{1}1]$ direction in *RE*Al-borates, forming a pseudolayered type of structure. From this point of view, therefore, striations on the trigonal prism faces correspond to boundaries between two phases with different *RE* concentrations. First of those phases, the polytype enriched in Y^{3+}, belongs to huntite $R32$ structure and the other, monoclinic ($C2$ or $C2/c$) modification, has high Gd(Nd) concentration.

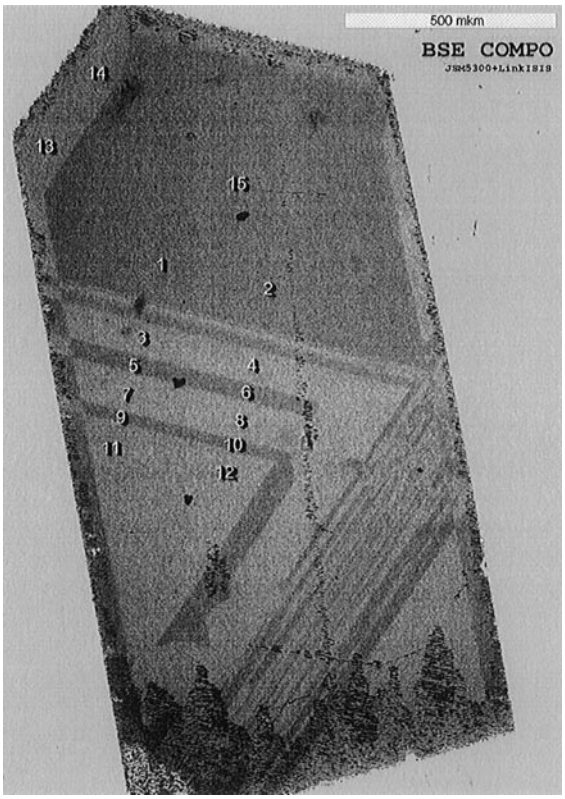

FIG. 2. Composition image of $(Gd_xY_{1-x})Al_3(BO_3)_4$ ($x = 0.75$).

The lattice constant for the NYAB and GYAB crystals with high neodymium and gadolinium concentration gradually changes with the crystal growth composition variations. All of these compounds belong to the *R*32 space group (Table 3).

TABLE 2
Microprobe Analysis of GYAB Crystals

Point number[a]	GYAB composition in fluxed melt	GYAB crystal composition	*K*
1	$Gd_{0.75}Y_{0.25}Al_3(BO_3)_4$	$Gd_{0.72}Y_{0.28}Al_3(BO_3)_4$	0.96
2		$Gd_{0.73}Y_{0.27}Al_3(BO_3)_4$	0.97
3		$Gd_{0.79}Y_{0.21}Al_3(BO_3)_4$	1.05
4		$Gd_{0.76}Y_{0.24}Al_3(BO_3)_4$	1.01
5		$Gd_{0.71}Y_{0.29}Al_3(BO_3)_4$	0.95
6		$Gd_{0.72}Y_{0.28}Al_3(BO_3)_4$	0.96
7		$Gd_{0.79}Y_{0.21}Al_3(BO_3)_4$	1.05
8		$Gd_{0.79}Y_{0.21}Al_3(BO_3)_4$	1.05
9		$Gd_{0.70}Y_{0.30}Al_3(BO_3)_4$	0.93
10		$Gd_{0.72}Y_{0.28}Al_3(BO_3)_4$	0.96
11		$Gd_{0.78}Y_{0.21}Al_3(BO_3)_4$	1.04
12		$Gd_{0.79}Y_{0.21}Al_3(BO_3)_4$	1.05
13		$Gd_{0.77}Y_{0.23}Al_3(BO_3)_4$	1.03
14		$Gd_{0.78}Y_{0.22}Al_3(BO_3)_4$	1.04
15		$Gd_{0.71}Y_{0.29}Al_3(BO_3)_4$	0.95

[a] Point numbers correspond to those in Fig. 2.

TABLE 3
Cell Parameters of GYAB and NYAB Crystals

Compound	*a* Å	α°
$Gd_{0.6}Y_{0.4}Al_3(BO_3)_4$	5.891(1)	104.33(2)
$Gd_{0.7}Y_{0.3}Al_3(BO_3)_4$	5.895(2)	104.34(2)
$Gd_{0.75}Y_{0.25}Al_3(BO_3)_4$	5.896(1)	104.32(2)
$Nd_{0.05}Y_{0.95}Al_3(BO_3)_4$	5.871(4)	104.32(3)
$Nd_{0.2}Y_{0.8}Al_3(BO_3)_4$	5.898(4)	104.26(3)
$Nd_{0.6}Y_{0.4}Al_3(BO_3)_4$	5.873(3)	104.33(1)
$Nd_{0.7}Y_{0.3}Al_3(BO_3)_4$	5.900(1)	104.28(1)
$Nd_{0.75}Y_{0.25}Al_3(BO_3)_4$	5.904(1)	104.29(5)

Some of LYAB crystals are inhomogeneous and they have strongly developed growth sectors (Fig. 3a) as well as growth bands (Fig. 3b). The light and dark areas on Fig. 3a correspond to the rombohedron and prism growth sectors, respectively. As it follows from the Table 4, the rombohedron growth sectors are reached by Lu in contrast to prism

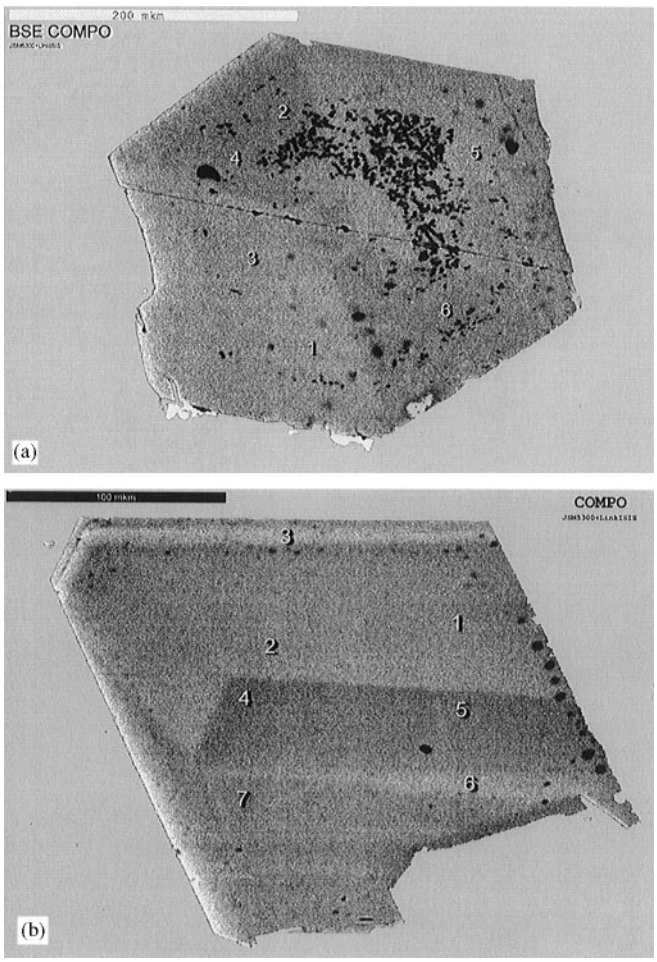

FIG. 3. Composition images of LYAB crystals: (a) $x = 0.05$, (b) $x = 0.025$.

TABLE 4
Microprobe Analysis of LYAB Crystals

Point number[a]	LYAB composition in fluxed melts	LYAB crystal composition	K
1	$(Lu_{0.05}Y_{0.95})Al_3(BO_3)_4$	$Lu_{0.049}Y_{0.951}Al_3(BO_3)_4$	0.98
2		$Lu_{0.046}Y_{0.954}Al_3(BO_3)_4$	0.87
3		$Lu_{0.053}Y_{0.947}Al_3(BO_3)_4$	1.0
4		$Lu_{0.038}Y_{0.962}Al_3(BO_3)_4$	0.72
5		$Lu_{0.053}Y_{0.947}Al_3(BO_3)_4$	1.0
6		$Lu_{0.037}Y_{0.953}Al_3(BO_3)_4$	0.70
1	$Lu_{0.025}Y_{0.975}Al_3(BO_3)_4$	$Lu_{0.020}Y_{0.980}Al_3(BO_3)_4$	0.8
2		$Lu_{0.023}Y_{0.977}Al_3(BO_3)_4$	0.92
3		$Lu_{0.024}Y_{0.976}Al_3(BO_3)_4$	0.97
4		$Lu_{0.016}Y_{0.984}Al_3(BO_3)_4$	0.65
5		$Lu_{0.018}Y_{0.979}Al_3(BO_3)_4$	0.70
6		$Lu_{0.024}Y_{0.976}Al_3(BO_3)_4$	0.94
7		$Lu_{0.017}Y_{0.983}Al_3(BO_3)_4$	0.68

[a] Point numbers correspond to those in Figs. 3a and 3b.

growth sectors. It is not excluded that these structural features depend on selective impurity trapping by different crystal growth sectors, but the growth bands correlate with fluctuations of crystal growth conditions.

CONCLUSION

Single crystals of *RE*YAB (*RE* = Nd, Gd, Ho, Yb, and Lu) were obtained from potassium trimolybdate based flux by spontaneous crystallization under various conditions. NGAB crystals have been grown using the TSSG method. Chemical composition of the grown crystals was determined, and the average *RE* effective segregation coefficients were calculated to be 0.35 and 1.02 depending on the *RE* type cations. The GYAB and NYAB unit cell parameters depend on the crystal compositions according to the Vegard rule.

ACKNOWLEDGMENTS

The research described in this paper was supported, in part, by Grant INTAS 97-515 and Russian Program "Integration" A0109-683. The authors thank V. N. Sokolov for the electron microscopy investigations and G. Bocelli and L. Righi for the structural investigations of grown crystals.

REFERENCES

1. A. D. Mills, *Inorg. Chem.* **1,** 960 (1962).
2. E. L. Belokoneva, M. A. Simonov, A. V. Pashkova, T. I. Timchenko, and N. V. Belov, *Dok. Akad. Nauk SSSR* **255,** 854 (1980). [in Russian]
3. E. L. Belokoneva, A. V. Pashkova, T. I. Timchenko, and N. V. Belov, *Dokl. Akad. Nauk SSSR* **261,** 361 (1981). [in Russian]
4. N. I. Leonyuk and L. I. Leonyuk, *Prog. Cryst. Growth Charact.* **31,** 179 (1995).
5. N. I. Leonyuk, *Prog. Cryst. Growth Charact.* **31,** 279 (1995).
6. L. M. Dorozhkin, I. I. Kuratev, N. I. Leonyuk, T. I. Timchenko, and A. V. Shestakov, *Pis'ma v ZhETF* **7,** 1297 (1981). [in Russian]
7. N. I. Leonyuk, V. V. Medved', N. I. Leonyuk, and S. N. Ivanov, "Acoustoelectronics, Varna, Bulgaria," Ext. Abstr. 459 (1989).
8. D. A. Keszler, A. Akella *et al. Mater. Res. Soc. Symp. Proc.* **329,** 15 (1994).
9. F. Kellendonk and G. Blasse, *J. Chem. Phys.* **75,** 561 (1981).
10. C. Gorller-Warland, E. Huygen, K. Binnemans, and L. Fluyt, *J. Phys. Conden. Matter* **6,** 7796 (1994).
11. G. Blasse, H. S. Kiliaan, and A. J. de Vries, *J. Lumin.* **40–41,** 639 (1988).
12. N. I. Leonyuk, A. V. Pashkova, and N. V. Belov, *Krist. Tech.* **14,** 47 (1979).
13. V. Nikolov and P. Peshev, *J. Cryst. Growth* **144,** 187 (1994).
14. S. T. Jung, D. Y. Choi, J. K. Kang, and S. J. Chung, *J. Cryst. Growth* **148,** 207 (1995).
15. X. B. Hu, S. S. Jiang, X. R. Huang, W. J. Liu, and C. Z. Ge *et al. J. Cryst. Growth* **173,** 460 (1997).
16. G. Wang, H. G. Gallagher, T. P. J. Han, and B. Henderson. *J. Cryst. Growth* **163,** 272 (1996).
17. E. L. Belokoneva and T. I. Timchenko, *Kristallografiya* **28,** 1118 (1983). [in Russian]